

Temporal measurements of surfactant squeeze-out from a surface using magnetically levitated liquid bridges

Neha M. Patel^a, P.L. Taylor^a, Michael R. Fisch^b, Charles Rosenblatt^{a,*}

^a *Department of Physics, Case Western Reserve University, Cleveland, OH 44106-7079, USA*

^b *Liquid Crystal Institute, Kent State University, Kent, OH 44242-0001, USA*

Received 31 July 2002; accepted 3 December 2002

Abstract

A cylindrical liquid bridge, laden with surfactant and constrained at the two ends by circular rods, was levitated against gravity in a magnetic field gradient. On axially translating one of the support rods to decrease the bridge's length, the axial electric resistance of the bridge was found to decrease. The relaxation time τ of the resistance as it approached its equilibrium value was measured as a function of surfactant concentration. Below the critical micelle concentration (CMC), we observed $\tau \sim 1$ s; above the CMC $\tau \sim 1.6$ s. The results are discussed in terms of capillary wave damping and surfactant squeeze-out from the surface.

© 2003 Elsevier Science B.V. All rights reserved.

Keywords: Dynamic surface tension; Surfactant; Liquid bridge; Microgravity

The “dynamic surface tension”, i.e., surface tension that varies with time [1–5], is critical to a number physiological and manufacturing processes. The conventional methods for measuring the dynamic surface tension in systems having length scales of hundreds of micrometers and larger are the Langmuir–Wilhelmy method, pendant drop or bubble, pulsating bubble surfactometry, and captive bubble tensiometry. The Langmuir–Wilhelmy method is based on a variable surface area Langmuir trough with a plate that monitors the surface tension [6]. This technique is useful for relatively low-density films, but it

does not permit rapid variation of the surface density with time. Pendant drops, and its inverse technique, pendant bubbles, involve shape changes over time as surfactants adsorb at the surface [7–13]. The technique may be performed in a transient manner or by oscillating the drop or bubble with time. This is similar to the pulsating bubble surfactometer, in which a small air bubble connected by a small tube to the outside is created within the surfactant solution [14]. The pressure in the bubble may be altered via this capillary tube, resulting in a change of bubble area. Repetition rates for this technique are limited to approximately 20 times per minute (0.33 Hz), and this technique is not accurate at high surfactant density (low surface tension) because the surfactant may be pushed into the capillary tube. Captive bubble

* Corresponding author.

E-mail address: cxr@po.cwru.edu (C. Rosenblatt).

tensiometry uses an isolated bubble floating against a hydrophobic agar gel inside a chamber [15]. Varying the pressure of the chamber changes the area of the bubble, which is measured and related to the surface tension. It is difficult to obtain high-frequency/large amplitude results with this technique and it is time consuming to modify the components of the surfactant solution.

The limitations of extant methods are especially critical when examining physiological fluids. For example, surfactants play an important role in modifying the surface tension of pulmonary fluids [16]. While surfactant synthesis is generally not a problem in healthy adults, it is a significant problem in adult cardiac patients, especially those with heart failure, and in neonates where the inability to synthesize sufficient lung surfactant is the cause of respiratory distress syndrome, which is a leading cause of death in premature babies [17]. In recent years, there has been considerable effort towards understanding and controlling the effects of surfactants and proteins in pulmonary liquids [16,18–20]. Since breathing involves an areal change of the fluid film that lines the lung's air sacs, understanding the dynamic surface tension of pulmonary fluids and their constituents is an urgent issue.

Given the importance of dynamic surface tension and the temporal inadequacy of current probes, alternative techniques that facilitate examination of processes that occur on faster time scales and that require only small volumes of fluid would be highly desirable. In this paper, we report a new microgravity approach that can be performed in either a simulated or real (space-borne) microgravity environment and that has the capability of yielding information about surfactant–fluid mixtures on time scales faster than 1 s and at high surfactant densities. Previously, a microgravity approach aboard the Space Shuttle Columbia was used to observe oscillations in surfactant-laden water droplets of approximately 2.3 cm in diameter [21]. Simulated microgravity has also been used, wherein quadrupolar shape oscillations were induced in acoustically levitated droplets [22]. Both these methods involved oscillations as opposed to transient phenomena. The basis of our new technique is an axially symmetric liquid bridge

that is levitated in air between two cylindrical support rods in a dynamically controlled, magnetically simulated low-gravity environment [23–26,30]; the bridge is then subjected to a sudden change in shape, and the electrical resistance across the bridge is measured as a function of time. Dynamics of liquid bridges in both real and simulated low-gravity environments (e.g., space-borne, ultrasonic and magnetic levitation, neutral buoyancy) have been studied extensively by various methods [25,31–38], including excitation of bridge vibration modes by movement of the cylindrical rods [31–35]. Here we apply the magnetic levitation method to a model fluid consisting of the cationic surfactant dodecyltrimethylammonium chloride (DTAC) dissolved in an aqueous paramagnetic liquid composed of $\text{MnCl}_2 \cdot 4\text{H}_2\text{O}$ and H_2O . Currently, we are utilizing two variants of our magnetically simulated low-gravity approach to the study of dynamic surface tension. In one experiment, we vary the magnetic field with time, and by doing so vary the total body forces on a surfactant-laden bridge and examine its resonance behavior [26]. In the method reported herein, we rapidly change the bridge length in a simulated near-zero gravity environment and examine its approach to equilibrium as a function of surfactant concentration.

When the length of a cylindrical liquid bridge is changed rapidly by translating one or both the rods along the cylinder's axis, it is the surface tension that drives the bridge to its new equilibrium shape; gravity is inconsequential due to the presence of the compensating magnetic body force. At or above the critical micelle concentration (CMC), an extension of the bridge, i.e., an increase in its length, temporarily decreases the concentration of surfactant at the surface. The bridge takes on an hourglass-like shape (actually a nodoid, a shape of constant mean curvature), reaching its equilibrium conformation on a time scale determined by the bulk viscous damping of capillary waves. On the other hand, a rapid decrease of bridge length temporarily increases the surfactant concentration at the surface. At low surfactant concentrations, the surface can easily accommodate the density change, and the time to reach equilibrium shape is again determined by viscous

damping of the induced capillary waves rather than by the time-varying surface tension. On the other hand, at or above CMC the higher surfactant density cannot be accommodated easily. In this regime, the relaxation time is determined by the removal of the surfactant from the surface into the bulk. The goal of this work is to test the magnetically levitated liquid bridge approach by measuring the expulsion time from the surface of a model surfactant when the relative decrease in bridge area is small. This avoids complications that may arise from multiple surface layers and layer collapse [27].

In order to have a fluid that can be levitated in a 10 kG laboratory magnet fitted with Faraday pole pieces, paramagnetic liquid mixtures were made with 62.5 wt.% $\text{MnCl}_2 \cdot 4\text{H}_2\text{O}$ + 37.5 wt.% water. Keeping the ratio of $\text{MnCl}_2 \cdot 4\text{H}_2\text{O}$ to water fixed, we then added a small amount of the cationic surfactant DTAC. This material was chosen as a model surfactant because its CMC occurs at concentrations that are varied easily while using small amounts of liquid. The concentration of DTAC is reported herein as a weight percent of the three-component mixture, and ranged from $X = 0$ to 1.5 wt.%. The density of the mixture was found to be 1.45 g cm^{-3} and the viscosity $1.6 \pm 0.1 \text{ cP}$. The static surface tension of the mixture was determined by the capillary rise technique. Results are shown in Fig. 1, where it is clear that CMC occurs at $X \approx 0.7\text{--}0.8 \text{ wt.}\%$.

Two cylindrical aluminum rods were machined with conical tips that served as wetting barriers for the liquid. The diameter of the tips was 0.4 cm. Each rod was mounted horizontally on a micro-translation stage, as shown in Fig. 2. This arrangement permitted adjustment of the slenderness ratio (ratio of the length of the liquid bridge to the initial diameter of the cylindrical liquid bridge) with fine precision. A programmable stepper motor was fixed under one of the translation stages to enable rapid movement of the rod, thereby facilitating rapid changes in the length of the liquid bridge.

A liquid bridge was constructed by injecting the paramagnetic mixture using a hypodermic needle into a small gap between the two rods. The magnetic field and gradient were adjusted so that

the upward magnetic force per unit volume $\chi H \nabla H$ just canceled the downward gravitational force [23–26,30], where χ is the magnetic susceptibility and H the magnetic field. The length of the bridge was then increased to an “initial” length $L_i = 1 \text{ cm}$ by withdrawing one of the rods and adding sufficient mixture so that the bridge assumed a cylindrical shape. Then, on translating the support rod and thereby shortening the cylindrical bridge from its starting length L_i , the bridge remained axisymmetric but bulged at the center. For aqueous bridges of order 1 cm in length and 4 mm in diameter, much of the shape change occurred nearly adiabatically on the time scale associated with the movement of the support rod, typically several hundred milliseconds. It is the shape change that occurred after the translation of the support rod has terminated in which we are interested. Because these final shape changes were very small compared with the dimensions of the bridge, optical imaging of the bridge was not a viable approach for these studies. Instead, we chose to make resistance measurements of the bridge, which are extremely sensitive to small variations in shape (see Fig. 2).

Fig. 3 shows the experimental arrangement used to measure the resistance of the liquid bridge. The entire bridge assembly was housed in a 100% humidity environment to prevent water evaporation. The bridge length was decreased by a distance $L_i - L_f = 0.13 \text{ cm}$ to its final length L_f in small but rapid steps (step size = $1.3 \times 10^{-4} \text{ cm}$, dwell time = 0.5 ms) over time $T = 500 \text{ ms}$, causing a decrease in its resistance and a bulge in shape. We approximate the form for the final ($t \rightarrow \infty$) equilibrium bridge radius as $r_f(z) = r_i + a \sin(\pi z / L_f)$, where $r_i = 0.2 \text{ cm}$ is the radius of the support rods (and therefore the radius of the initial cylindrical bridge). The volume of the bridge was unchanged during and after the translation of the support rod, and is given by

$$\Omega_i = \pi r_i^2 L_i = \int_{z=0}^{L_f} \pi r_f(z)^2 dz. \quad (1)$$

Thus, for $a \ll r_i$, we find that $a \approx \pi r_i (L_i - L_f) / 4 L_f \approx 0.023 \text{ cm}$. The initial area of the air–fluid interface was $A_i = 2\pi r_i L_i$; the final surface area was $A_f = 2\pi \int_{z=0}^{L_f} r_f(z) dz$. Therefore, we find a change in

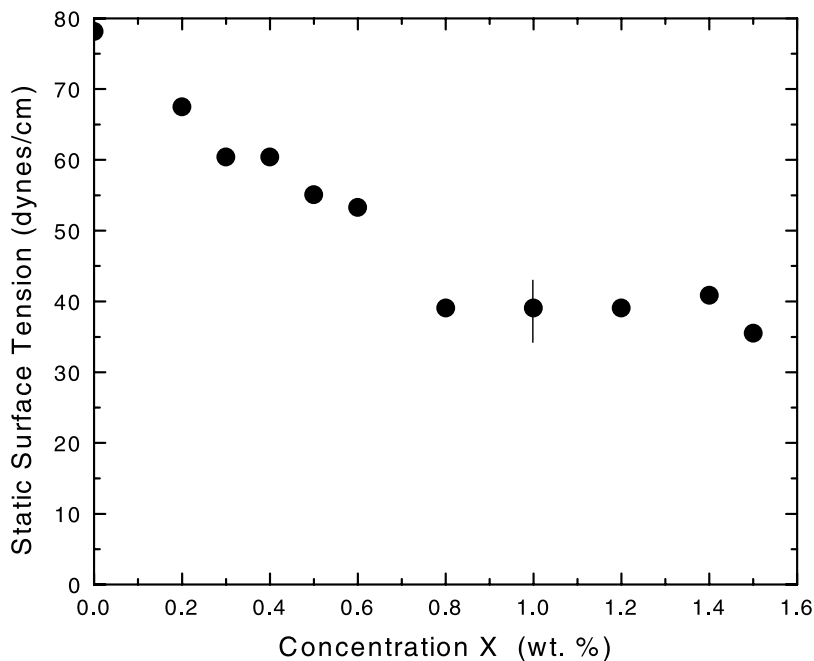


Fig. 1. Schematic diagram of experimental setup (top view). The liquid bridge is supported by two conically machined aluminum rods.

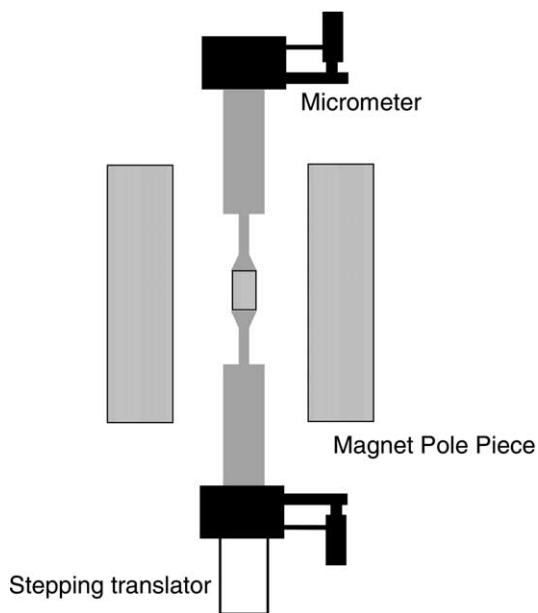


Fig. 2. Static surface tension vs. surfactant concentration. Notice that CMC occurs at $X \sim 0.7$. Typical error bar is shown.

surface area $A_f - A_i \approx 2\pi r_i(L_f - L_i) + 4aL_f \approx -0.123 \text{ cm}^2$, and the fractional area change was

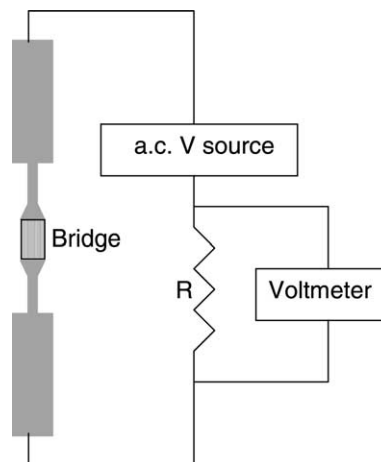


Fig. 3. Schematic diagram of experimental setup to measure electrical resistance.

$(A_f - A_i)/A_i = -0.098$. Thus the area decreased as the bridge length was reduced.

An a.c. voltage of $V_S = 0.5 \text{ V r.m.s.}$ at 1 kHz was applied, and the voltage drop V_R across the series resistor ($R_R = 100 \ \Omega$) was measured using a Keithley Model 2000 digital voltmeter. (The voltmeter had a sharp frequency cutoff at approxi-

mately $f_{\text{cutoff}} = 6$ Hz. For input voltages at frequency $f > f_{\text{cutoff}}$ the voltmeter output was a d.c. signal that corresponded to the true r.m.s. voltage. If the amplitude of a sinusoidal input voltage varied at frequency $f < f_{\text{cutoff}}$, the voltmeter's output followed the slowly varying r.m.s. input voltage. The parameter f_{cutoff} will be important in analyzing our measurements.) The final equilibrium resistance of the bridge, $R_B^f = R_B^i + \Delta R_B$, was of order 200 Ω . Here $R_B^i = \rho L_i / \pi r_i^2$ is the resistance of the initial cylindrical bridge, ρ the resistivity of the fluid and ΔR_B the decrease in the bridge's resistance due to the reduction in its length and is given by

$$\Delta R_B = \int_{z=0}^{L_f} \frac{\rho}{\pi r_f(z)^2} dz - \frac{\rho L_i}{\pi r_i^2}. \quad (2)$$

The instantaneous measured voltage V_R across the resistor, which is a function of time, is

$$V_R \approx V_S \frac{R_R}{R_R + R_B^{\text{inst}}}. \quad (3)$$

Here, R_B^{inst} is the instantaneous bridge resistance (which decreases to R_B^f as $t \rightarrow \infty$). The voltage V_R was recorded at time intervals of 0.2 s beginning several seconds before the length of the bridge was changed, through the decrease in bridge length to L_f , and for several seconds thereafter. The change in measured voltage δV_R was found experimentally to be of opposite sign and to lowest-order linear in the bridge's resistance change ΔR_B , consistent with Eq. (3). The process was repeated at least five times at each surfactant concentration. A typical trace of V_R vs. time is shown in Fig. 4. We note that the voltage V_R , and thus the initial resistance, were approximately independent of the surfactant concentration. The first 500 ms of the rise in V_R vs. time correspond to the bridge's gross change of shape on decreasing its length. Once the bridge's length reached $L_f = 0.87$ cm and no longer changed with time, there remained a small exponential change in V_R . It is this exponential piece of δV_R that we wish to examine.

Fig. 5 shows the relaxation time τ of the exponential tail as a function of surfactant concentration. Reported values for τ correspond to an average over many experimental runs at each

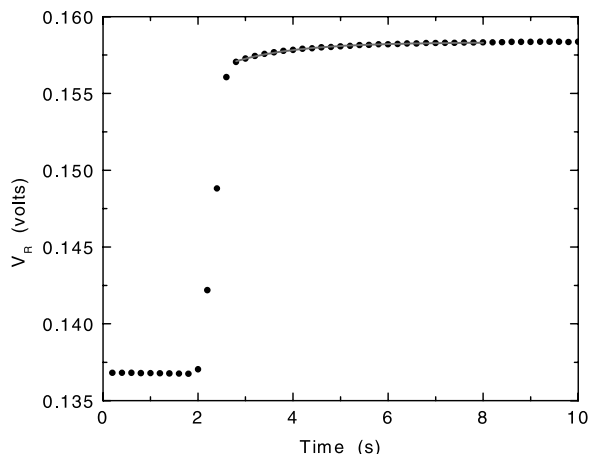


Fig. 4. Typical trace of V_R vs. time. Rapid rise occurs during the $T = 500$ ms translation of support rod, followed by exponential relaxation. The solid curve represents a single exponential fit to the relaxation.

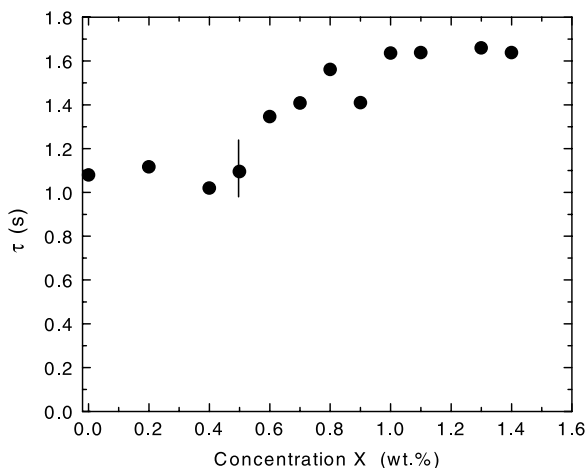


Fig. 5. Relaxation time τ vs. concentration. Typical error bar is shown.

concentration, with typical error bars shown. For $X \lesssim 0.5$ wt.% we find $\tau \sim 1.0$ s; for $X \gtrsim 0.8$ wt.% we find $\tau \sim 1.6$ s. There is a smooth transition from the low-density to the high-density regime. Not surprisingly, CMC resides in the crossover region (cf. Fig. 1).

We believe that a different process contributes to the measured relaxation time in each of the two regions. For concentrations below CMC, the bridge rapidly reached its near-equilibrium shape,

subject only to capillary oscillations created during the movement of the support rod; gravity was not an issue for the magnetically levitated bridge. To understand the effect of these oscillations on our resistance measurements, we intentionally induced oscillations of much larger amplitude and examined them optically. If we assume that the instantaneous radius $r(z) = r_f(z) + \delta r(z)$ locally oscillates about, and is damped toward, the equilibrium radius $r_f(z)$, the difference between the instantaneous bridge resistance R_B^{inst} and its final equilibrium value R_B^f may be obtained by substituting $r(z)$ into $R_B^{\text{inst}} = \int_{z=0}^{L_f} \rho / [\pi r(z)^2] dz$ and expanding for small $\delta r(z)$:

$$R_B^{\text{inst}} - R_B^f \approx \int_{z=0}^{L_f} \frac{\rho}{\pi r_f(z)^2} \times \left[-2 \frac{\delta r(z)}{r_f(z)} + 3 \left(\frac{\delta r(z)}{r_f(z)} \right)^2 - 4 \left(\frac{\delta r(z)}{r_f(z)} \right)^3 + \dots \right] dz. \quad (4)$$

First, notice that all even power terms are positive. Additionally, due to conservation of volume, local negative deviations $\delta r(z)$ from $r_f(z)$ that result in a constriction of the bridge must be larger in magnitude than positive deviations that result in a locally larger radius. Thus $R_B^{\text{inst}} - R_B^f > 0$, which implies that the average resistance would continue to decrease as the oscillations are damped. This was as observed experimentally. It turns out that the oscillation frequencies, which depend on surface tension and therefore surfactant concentration, were observed to be of order 8 Hz for the higher concentration mixtures above CMC, and faster for the lower concentration mixtures. This is consistent with the frequencies observed for the lowest symmetric capillary modes driven with modulated ultrasonic radiation pressure [28]. Thus, these oscillations were sufficiently rapid and damped sufficiently slowly that, by design, the a.c. voltmeter reported only the relaxation of the r.m.s. amplitude; this resulted in a smooth trace in Fig. 4. Moreover, in the underdamped limit, the relaxation time is predicted to be proportional to the viscosity divided by the density. Thus τ should be independent of surfac-

tant concentration, again as observed. Finally, we remark that the fast oscillation frequency f depends on surface tension and therefore on the surfactant absorption/desorption mechanism. Because $f > f_{\text{cutoff}}$, we did not observe the oscillations in our experiments for low surfactant concentrations.

We believe that a different relaxation mechanism occurs for concentrations well above CMC. As calculated above, the surface area of the bridge decreased by nearly 10% as the bridge length was varied from L_i to L_f . It is well known that the damping of capillary waves increases sharply on approaching CMC [29], often by as much as 10-fold. This would result in a rapid decrease in the relaxation time and, other things being equal, the shape of the bridge and the resulting resistance very rapidly would reach their equilibrium values. However, it is clear from Fig. 5 that the relaxation time increases rather than decreases above the CMC. As noted earlier, studies of dynamic surface tension are generally performed over a complete compression/decompression cycle of large amplitude. A consequence of this is that it may be necessary to incorporate layer collapse and sublayers [27] to model adequately the observed experimental hysteresis curves. However, for smaller areal changes, one may consider desorption and surfactant “squeeze-out” as the operative mechanisms [27,39–41], depending upon the initial and final concentrations. Under these circumstances, our bridge (above CMC) begins with its maximum equilibrium surface concentration. On translation of the support rods, the bridge adopts a near-equilibrium shape, with vibration-induced capillary waves already having decayed away and no longer playing an important role. As the bridge’s instantaneous surface area is smaller than its initial area A_i , the surfactant concentration at the surface has temporarily increased. Desorption may take place, although it has been suggested [40] and supported experimentally [39] that for small compressions above the maximum equilibrium surface concentration the surfactant molecules at the surface are not exchanged with the bulk. In this region, neither adsorption nor desorption takes place. When the area is further decreased, the dynamic surface tension reaches a

minimum, and any further decreases in area result in a squeezing-out of surfactant from the surface into the bulk [39–41]. The squeeze-out of surfactant is rapid (order of seconds) [39], certainly much faster than typical desorption times of tens of seconds [40]. However, as the expulsion of surfactant into the bulk occurs on time scales slower than the translation time T of the support rod, the surface area initially remains larger than its final equilibrium area A_f . During squeeze-out the surface tension initially will be non-uniform, since the surfactant layer will be most compressed in the region near the moving support rods. As the surface tension approaches its uniform value, the shape of the liquid surface becomes more symmetric, and the resistance decreases. The time τ measured above the CMC therefore would reflect this squeezing-out process. One can define a dimensionless surfactant depletion depth $\lambda = \Gamma_\infty / Cr_i$ [27], where Γ_∞ is the maximum equilibrium surface concentration of surfactant and C the bulk surfactant concentration in units of cm^{-3} . For concentrations corresponding to $X \sim 1$ wt.%, we find $C \sim 1.6 \times 10^{19} \text{ cm}^{-3}$. Using the Gibbs isotherm, $\Gamma_\infty = -(\text{d}\gamma/\text{d} \ln C)/k_B T$, where γ is the surface tension, T the temperature and k_B Boltzmann's constant, from Fig. 2 we estimate $\Gamma_\infty \sim 3 \times 10^{13} \text{ cm}^{-2}$, resulting in $\lambda \sim 10^{-5} \ll 1$. The characteristic time τ_d for diffusion from the surface is of order the $\lambda^2 r_i^2 / D$, where D is the diffusion constant. Since $D \sim 1.6 \times 10^{-8} \text{ cm}^2 \text{ s}^{-1}$ [27], we find τ_d to be of order 10^{-4} s . This is much faster than the measured values of τ (cf. Fig. 5), which indicates that the observed process is not diffusion limited, as expected [27]; rather τ corresponds to the time required to remove the surfactant molecules from the surface. These conclusions, moreover, are valid even if our estimate for Γ_∞ was too small by an order of magnitude. Because τ seems to be nearly independent of X above CMC, our data would indicate that the reservoir's density would not be so large that it would impede further removal of surfactant from the surface. Additionally, because of the relatively small areal change, we do not expect there to be a complete subsurface double-layer [27] on compression, although regions of such subsurface layers may exist.

We note that we have not examined a complete cycle of compression/expansion. As the expansion of a bridge in equilibrium has the effect of decreasing the surfactant concentration below CMC, the resistance would be dominated by capillary waves, as it is on compression in the low surfactant regime. Thus, our technique would not supply useful information about readsorption of surfactant.

Although our technique does not facilitate measurement of the surface tension, it is able to provide important information about the time scales associated with surfactant exchange between bulk and surface. Using a model surfactant, we have observed a clear change in time scale that occurs around CMC, and have related the data above CMC to the removal of surfactant from the surface due to compression. Modifications of the apparatus will facilitate measurements on shorter time scales and at higher concentrations. One issue that needs to be addressed is the effect of the high concentrations of $\text{MnCl}_2 \cdot 4\text{H}_2\text{O}$ on the transport of surfactant and formation of micelles. We are unaware of either theoretical or experimental results that address this issue. Experimentally, at least, we intend to examine mixtures with reduced $\text{MnCl}_2 \cdot 4\text{H}_2\text{O}$ but at higher magnetic fields in order to gauge its effects. Ultimately, it will be necessary to perform the experiment in a sufficiently high magnetic field or in a space-borne environment to obviate the need for $\text{MnCl}_2 \cdot 4\text{H}_2\text{O}$ in the mixture.

Acknowledgements

The authors thank Prof. J.I.D. Alexander for useful discussions. This work was supported by the National Aeronautics and Space Administration under grant NAG8-1779.

References

- [1] T. Horozov, L. Arnaudov, J. Colloid. Interf. Sci. 219 (1999) 99.
- [2] C.T. Hsu, C.H. Chang, S.Y. Lin, Langmuir 16 (2000) 1211.

- [3] S. Manning-Benson, S.R.W. Parker, C.D. Bain, R.C. Darton, D. Sharpe, J. Eastoe, P. Reynolds, *Langmuir* 13 (1997) 5808.
- [4] S. Manning-Benson, S.R.W. Parker, J. Penfold, *Langmuir* 14 (1998) 990.
- [5] J.K. Ferri, K.J. Stebe, *Adv. Colloid. Interf. Sci.* 85 (2000) 61.
- [6] J. Clements, *Proc. Soc. Exp. Biol. Med.* 95 (1957) 170.
- [7] D.O. Johnson, K.J. Stebe, *J. Colloid. Interf. Sci.* 182 (1996) 526.
- [8] J.K. Ferri, S.Y. Lin, K.J. Stebe, *J. Colloid. Interf. Sci.* 241 (2001) 154.
- [9] H.C. Chang, C.T. Hsu, S.Y. Lin, *Langmuir* 14 (1998) 2476.
- [10] C. Ybert, J.M. DiMeglio, *Langmuir* 14 (1998) 471.
- [11] I. Nahrngbauer, *J. Colloid. Interf. Sci.* 176 (1995) 318.
- [12] S.Y. Park, C.H. Chang, D.J. Ahn, E.I. Franses, *Langmuir* 9 (1993) 3640.
- [13] B. Persson, S. Nilsson, R. Bergman, *J. Colloid. Interf. Sci.* 218 (1999) 433.
- [14] G. Enhorning, *J. Appl. Physiol. Respiratory, environmental and exercise physiology* 43 (1977) 198.
- [15] S. Schurch, H. Bachofen, J. Goerke, F. Possmeyer, *J. Appl. Physiol.* 67 (1989) 1425.
- [16] R. Veldhuizen, K. Nag, S. Orgeig, F. Possmayer, *Biochim. Biophys. Acta* 1408 (1998) 90 (See review by).
- [17] D.L.A. Wyncoll, T.W. Evans, *Lancet* 354 (1999) 497.
- [18] R.J. King, J.A. Clements, *Am. J. Physiol.* 223 (1972) 715.
- [19] Z. Wang, S.B. Hall, R.H. Notter, *J. Lipid Res.* 36 (1995) 1283.
- [20] A. Gopal, K.Y.C. Lee, *J. Phys. Chem. B* 105 (2001) 10348.
- [21] R.E. Apfel, Y. Tian, J. Jankovsky, T. Shi, X. Chen, R.G. Holt, E. Trinh, A. Croonquist, K.C. Thornton, A. Sacco, C. Coleman, F.W. Leslie, D.H. Matthiesen, *Phys. Rev. Lett.* 78 (1997) 1912.
- [22] Y. Tian, R.G. Holt, R.E. Apfel, *J. Colloid. Interf. Sci.* 187 (1997) 1.
- [23] M.P. Mahajan, S. Zhang, M. Tsige, P.L. Taylor, C. Rosenblatt, *J. Colloid. Interf. Sci.* 213 (1999) 592.
- [24] M.P. Mahajan, M. Tsige, P.L. Taylor, C. Rosenblatt, *Phys. Fluids* 10 (1998) 2208.
- [25] M.P. Mahajan, M. Tsige, J.I.D. Alexander, P.L. Taylor, C. Rosenblatt, *Phys. Rev. Lett.* 84 (2000) 338.
- [26] M.P. Mahajan, M. Tsige, S. Zhang, J.I.D. Alexander, P.L. Taylor, C. Rosenblatt, *Exp. Fluids* 33 (2002) 503.
- [27] M.A. Krueger, D.P. Gaver, *J. Colloid. Interf. Sci.* 229 (2000) 353.
- [28] S.F. Morse, D.B. Thiessen, P.L. Marston, *Phys. Fluids* 8 (1996) 3.
- [29] T.J. Asaki, D.B. Thiessen, P.L. Marston, *Phys. Rev. Lett.* 75 (1995) 2686.
- [30] N.M. Patel, M.R. Dodge, L.A. Slobozhanin, J.I.D. Alexander, P.L. Taylor, C. Rosenblatt, *Phys. Rev. E.* 65 (2002) art. No. 026306.
- [31] J. Meseguer, A. Sanz, *J. Fluid Mech.* 153 (1985) 83.
- [32] A. Sanz, *J. Fluid. Mech.* 156 (1985) 101.
- [33] A. Sanz, J.L. Diez, *J. Fluid Mech.* 205 (1989) 503.
- [34] J.M. Perales, J. Meseguer, *Phys. Fluids A* 4 (1992) 1110.
- [35] D.J. Mollot, J. Tsamopoulos, T.Y. Chen, N. Ashgriz, *J. Fluid Mech.* 255 (1993) 411.
- [36] J. Tsamopoulos, T.Y. Chen, A. Borkar, *J. Fluid Mech.* 225 (1992) 579.
- [37] Y. Zhang, J.I.D. Alexander, *Phys. Fluids A* 2 (1990) 1966.
- [38] B.J. Lowry, P.H. Steen, *J. Colloid. Interf. Sci.* 170 (1995) 38.
- [39] J. Goerke, J.A. Clements, in: *Handbook of Physiology. The Respiratory System, Mechanics of Breathing*, Am. Physiol. Soc. Sect. 3, Vol. III, Part 1, 1986, p. 247.
- [40] D.R. Otis, E.P. Ingenito, R.D. Kamm, M. Johnson, *J. Appl. Physiol.* 77 (1994) 2681.
- [41] P. Tchoreloff, A. Gulik, B. Denizot, J.E. Proust, F. Puisieux, *Chem. Phys. Lipids* 59 (1991) 151.